Catalysis Today 146 (2009) 2–8

Contents lists available at ScienceDirect

Catalysis Today

journal homepage: www.elsevier.com/locate/cattod

The effect of water on direct ethanol molten carbonate fuel cell

Hary Devianto [a], Zhenlan Li [a], Sung Pil Yoon [b], Jonghee Han [b], Suk-Woo Nam [b], Tae-Hoon Lim [b], Ho-In Lee [a,*]

[a] School of Chemical and Biological Engineering & Research Center for Energy Conversion and Storage, Seoul National University, 599 Gwanangno, Gwanak-gu, Seoul 151-744, Republic of Korea
[b] Center for Fuel Cell Research, Korea Institute of Science and Technology, 39-1 Hawolgok-dong, Seongbuk-gu, Seoul 136-791, Republic of Korea

ARTICLE INFO

Article history:
Available online 23 January 2009

Keywords:
MCFC
Ethanol
Water effect
Recycling
Corrosion

ABSTRACT

Bio-ethanol can be used directly as a fuel in molten carbonate fuel cell (MCFC). Unfortunately, the high water content of bio-ethanol has several negative effects; decrease in performance, electrolyte loss due to evaporation, and corrosion of anode cell frame. This research was conducted to overcome the negative effects without degrading MCFC's performance and stability. A decrease in performance due to low H_2 contents was unavoidable. An electrolyte loss was minimized when the recycling method was used. The optimum recycling ratio was achieved when the flow rate ratio of output to recycle was in the range of 0.7–1. A corrosion of the cell frame was successfully blocked by Ni-electroplated cell frame. This system was successfully tested for over 2000 h without any decrease in performance.

1. Introduction

Molten carbonate fuel cell (MCFC) is one of the promising candidates for future power generation. The highest performance is achieved when hydrogen is used as a fuel. However, insufficient hydrogen infrastructure leads to the high price of hydrogen. Bio-ethanol with H_2O:EtOH = 13 (by mol), is a kind of ethanol which is produced from the fermentation of sugarcane, corn, or other biomass sources. By creating steam reforming reaction inside the MCFC anode chamber, this bio-ethanol can be used directly as a fuel [1].

Unfortunately, the high water content of bio-ethanol has several negative effects; decrease in performance, electrolyte loss due to evaporation, and corrosion of anode cell frame. This research was conducted to overcome the previous phenomena without degrading MCFC's performance and stability.

There are some facts on corrosion in molten carbonate fuel cell system; corrosion can cause electrolyte loss more than 20% of the total amount during operation [3], corrosion rate is higher at the anode side than at the cathode side [4], and water is regarded as the oxidizing agent at the anode side [5]. In order to eliminate the effect of corrosion, Ni electroplating and Ni electroless plating were employed since nickel is considered to be most thermodynamically stable in anode environment [3].

Electroplating is a process by which a metal in its ionic form is supplied with electrons to form a non-ionic coating on a desired substrate. The most common system involves: a chemical solution which contains the ionic form of the metal, an anode (positively charged electrode) which may consist of the metal being plated (a soluble anode) or an insoluble anode (usually carbon, platinum, titanium, lead, or steel), and finally, a cathode (negatively charged electrode) where electrons are supplied to produce a film of non-ionic metal. On the other hand, electroless plating, also known as chemical or auto-catalytic plating, is a non-galvanic type of plating method that involves several simultaneous reactions in an aqueous solution which occur without the use of external electrical power. The reaction is accomplished when hydrogen is released by a reducing agent, normally sodium hypophosphite, and oxidized; thus, producing a negative charge on the surface of the part.

2. Experimental

2.1. Surface modification of MCFC anode

In order to improve the single cell test performance, a catalyst should be coated on the anode; thus, it can help the anode to enhance its activity on ethanol steam reforming. The conventional MCFC anode was a highly porous sintered-nickel powder of "chain" morphology type (INCO #255) alloyed with chromium. It was prepared through a procedure involving tape casting, drying, and calcination of a slurry mixture of solvent (water), binder (methyl cellulose #1500; Junsei Chemical Co., Japan), plasticizer

* Corresponding author. Tel.: +82 2 880 7072; fax: +82 2 888 1604.
E-mail address: hilee@snu.ac.kr (H.-I. Lee).

0920-5861/$ – see front matter © 2009 Elsevier B.V. All rights reserved.
doi:10.1016/j.cattod.2008.12.017

(glycerol; Junsei Chemical Co., Japan), defoamer (SN-154; San Nopco, Korea), deflocculant (cerasperse-5468; San Nopco, Korea), and Ni powder (INCO #255; particle size: 3 μm), as reported previously [6].

15 wt% Ni/MgO was hot-pressed onto a Ni substrate. The hot-pressing method is used because of its simple process, ease of control in the uniformity of the coating layer without the use of expensive equipments, and high selectivity due to one-side layer fabrication [2]. We prepared hot pressing method by mixing binder, plasticizer, homogenizer, dispersant with the catalyst powder in the presence of ethanol and water as a mixed solvent. Paste-like catalyst was prepared through ball milling and deairing process for 2 h until the viscosity reached 5000 cp. The coated anode prepared was dried at 120 °C for 3 h and heat treated at 300 °C in air for 3 h prior to the activity test in order to remove the organic material. The 5 wt% catalyst-coated anode was prepared to evaluate the effect of water partial pressure in the anode chamber [7].

2.2. Single cell test

A set of experiment for single cell (10 cm × 10 cm) test was prepared to evaluate the performance of the coated anode towards time. The prepared samples were placed in the heating block with cathode, electrolyte, matrix, current collector, and cell frame to form a single molten carbonate fuel cell. The characteristics of the single cell components are summarized in Table 1. A pressure of 2 kg_f/cm^2 was applied to the single cell using an air cylinder. Operation of a single cell having a 10 cm × 10 cm anode was performed after pretreatment at temperatures from 25 to 450 °C for 3 days in air and then from 450 to 650 °C for 3 days in CO_2. Under the latter conditions which were critical to electrolyte melting region, CO_2 was passed through the system at a low flow rate to maintain the distribution of the electrolyte throughout the pores of the matrix, cathode, and anode, and also to prevent evaporation of the electrolyte. After pretreatment, the temperature of the gas in the MCFC maintained at 650 °C for 180 h, followed by a mixture of bio-ethanol with N_2 as a carrier gas being introduced. The anode gas consisted of H_2, CO_2, and H_2O in a 72:18:10 mole ratio; the cathode gas consisted of air and CO_2 in a 70:30 mole ratio. During the introduction of bio-ethanol, the *I–V* curve was measured under bio-ethanol as a fuel. Open circuit voltage (OCV), performance, and internal resistance were all measured during cell operation.

Table 1
Characteristics of single cell components.

Unit cell components	Values and characteristics
Cell frame of anode and cathode	
Size (width × length; cm × cm)	13 × 13
Material	SS316L (aluminized on the wet seal area)
Anode electrode and current collector	
Size (width × length; cm × cm)	11 × 11
Material (electrode; current collector)	Ni–10 wt% Cr; Ni
Mole% of fuel gas ($H_2/CO_2/H_2O$)	72/18/10
Total flowrate	950 ccm
Cathode electrode and current collector	
Size (width × length; cm × cm)	10 × 10
Material (electrode; current collector)	In situ lithiated NiO; SUS 316
Mole% of fuel gas (Air/CO_2)	70/30
Total flowrate	365 ccm
Catalyst	
Material	15 wt% Ni/MgO
Amount	5 wt% anode
Electrolyte	
Li_2CO_3/K_2CO_3 mole ratio	62/38
Matrix	γ-$LiAlO_2$
Mass ratio of electrolyte to matrix (%)	108–110%

2.3. Characterization

Several different analysis techniques were employed to examine the characteristics of the prepared samples. The surface morphology and the magnesium depth distributions of the porous catalyst-coated Ni–10 wt% Cr anode were explored using scanning electron microscopy (SEM; Philips XL30 ESEM) in conjunction with energy dispersive spectrometry (EDAX). The pore size distribution was analyzed using an Hg porosimeter (Micromeritics Autopore IV). The porosity of the sample was calculated using the Archimedes principle (ASTM C373-88). CHNS and induced coupled plasma–atomic emission spectroscopy (ICP-AES) analyses were carried out to evaluate the trace components in the system.

3. Results and discussions

This research originated from the experiment regarding durability test of direct ethanol MCFC as shown in Fig. 1. The catalyst-coated anode worked perfectly for at least 2000 h under bio-ethanol atmosphere which consisted of 20 vol% of EtOH in aqueous solution [2]. Unfortunately, there was a significant loss in performance when the cell operated for 3000 h. The voltage drop became obvious, followed by an increase in both N_2 crossover and ohmic resistance indicating that there was a substantial amount of electrolyte loss in the single cell. Post test of dissembling the cell confirmed the loss of electrolyte and found that the severe corrosion occurred on the cell frame of anode chamber where it contacted directly with bio-ethanol. Electrochemical impedance spectroscopy (EIS) spectra suggested an increase in ohmic polarization representing the electrolyte loss problem as shown in Fig. 1. The experiment confirmed that the previous data indicated considerable losses of voltage and electrolyte due to high partial pressure of water and the cell frame corrosion [2]. To simplify the discussion, this topic is divided into two parts, the first is the effect of partial pressure of water and the second is the effect of corrosion.

3.1. The effect of partial pressure of water

To evaluate the effect of partial pressure of water on the cell performance, we obtained the initial *I–V* curve of a single cell with various water contents. The results only showed slight difference

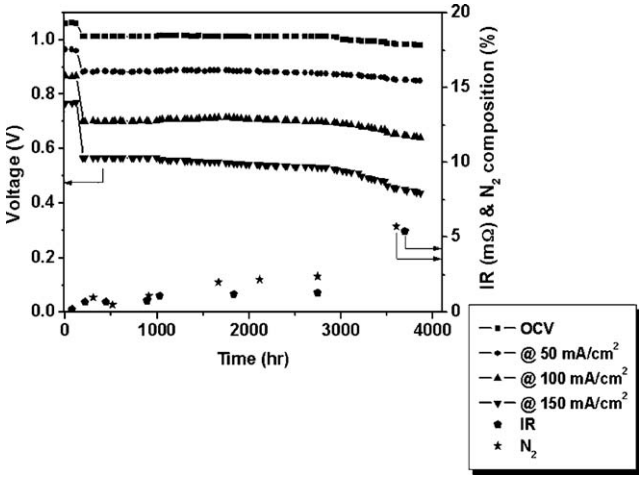

Fig. 1. Durability test of direct ethanol MCFC having catalyst-coated anode.

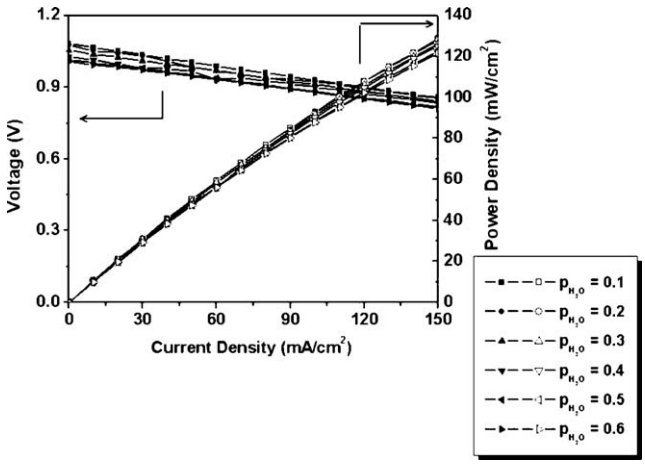

Fig. 2. Initial *I–V* curve for various partial pressures of water.

in performance, but obvious changes were observed when the EIS spectra were analyzed, as shown in Fig. 2. The decrease in performance was observed with the increase in partial pressure of water. The slopes of *I–V* curve at different partial pressure are relatively similar. An increase in water content influenced mainly to mass transfer polarization. The water contents affected directly the value of OCV. The higher the water contents, the lower the OCV. As OCV represents the amount of products at the equilibrium state, the amount can be calculated from Nernst equation.

Closed circuit potential (CCP) at 150 mA/cm^2 indicated a similar trend. At high current density, high amount of water is produced resulting in an additional barrier for anode reactant gas. In order to reach triple phase boundary, where gas, solid, and electrolyte can all react one another, H_2 in this case should face the previous barrier. This phenomenon is confirmed by an increase in mass transfer polarization quoted from Nyquist plot of EIS data (Fig. 3).

The EIS analysis was carried out to investigate the cell phenomena without damage of the cell. Nyquist plot shows no significant change in ohmic resistance and charge transfer resistance. Ohmic resistance is represented by the initial value of the first loop arc intercepted to the *x*-axis of Z real part (Fig. 3). This ohmic resistance is influenced mainly by the amount of resistance caused by contact between components or lack of electrolyte. The charge transfer resistance indicated by the first semicircle is evident in all variations.

The only obvious difference was shown in mass transfer resistance, which is the second semicircle of the graph. With the increase in partial pressure of the water, the second semicircle became larger indicating higher mass transfer polarization. This

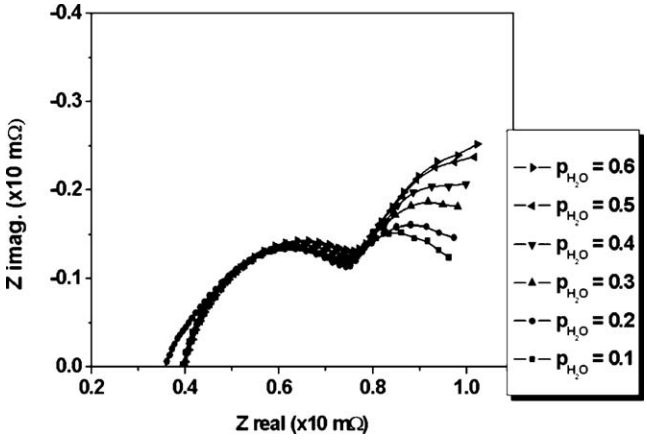

Fig. 3. Initial Nyquist plots of various water contents.

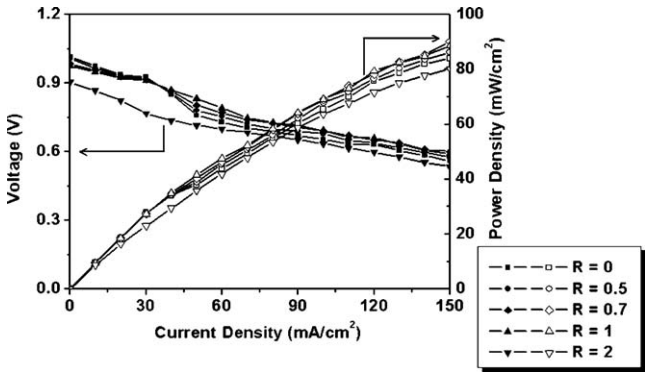

Fig. 4. Initial *I–V* curves of various recycling ratios.

phenomenon can be explained by huge amount of water blocking the H_2 diffusion at the anode chamber.

Several solutions have been carried out, but the best one came from the recycling system. The idea of this system is to reduce the partial pressure of water at the single cell inlet by letting some part of the gas product be mixed with the initial reactant at a certain ratio. Recycling ratio is defined as:

$$R = \frac{\text{Recycling flow rate}}{\text{Output flow rate}}$$

Various recycling ratios were investigated to obtain the optimum condition (Fig. 4). Low recycling ratio did not affect much the partial pressure of water; on the other hand high recycling ratio dropped the amount of hydrogen produced from steam reforming of bio-ethanol, and thus, the equilibrium state shifted to the left. Eventually it led to the low performance of the cell. The optimum recycling ratio was achieved at the ratio between 0.7 and 1, where the flow rate of recycling is almost similar to that of gas output.

3.2. The effect of corrosion on the cell frame

Another problem occurred on the stainless steel cell frame at the anode chamber. High water content yielded corrosion on the cell frame, since it acted as an oxidizing agent in anodic atmosphere. This oxide layer could react with the electrolyte and also block electron pathway to the external circuit [3]. Recycling system decreased the corrosion to some extent by low water content at the anode chamber. However, it is not sufficient to eliminate the effect of corrosion, particularly in the long term. Analyses on pore size distribution, mean pore size, and porosity using mercury porosimetry and ASTM C373-88 method indicated the effects of catalyst-coated anode such as lower mean pore size and porosity in comparison with as-prepared anode (Fig. 5 and

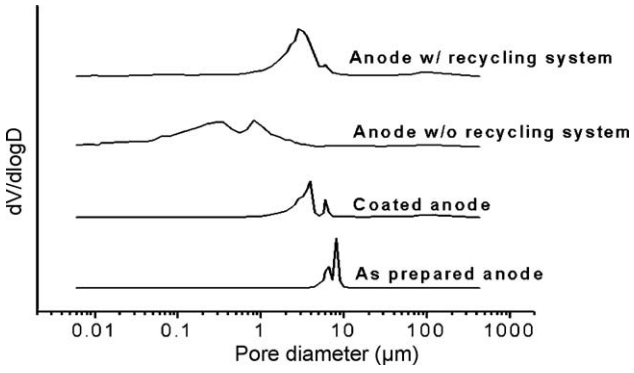

Fig. 5. Pore size distribution of anodes operated under recycling system.

Table 2
Mean pore size and porosity of anode under recycling system.

Sample	Mean pore size[a] (μm)	Porosity[b] (%)
Anode with recycling system	2.4	40.3
Anode with out recycling system	1.1	33.1
Catalyst-coated anode	2.8	46.4
As prepared anode	5.7	60.2

[a] Mercury porosimetry.
[b] ASTM C373-88.

Table 2). When the anode operated under recycling system for 1000 h was compared with the fresh catalyst-coated anode, the pore size distribution curve did not change significantly. However, slight decreases in pore size and porosity were observed. On the other hand, the anode which was exposed without the recycling system for the same period of time (1000 h) showed obvious differences; such as, much lower pore size and porosity. High partial pressure of water seemed to play an important role of the oxidation phenomenon at the anode.

In order to avoid or completely remove the corrosion phenomena, coating material over SUS cell frame was proposed. Ni has an advantage as it is a thermodynamically stable material in anode environment; thus, it is suitable for this purpose [8]. Both Ni electroless plating and Ni electroplating methods were used to overcome the effect of corrosion. Fig. 6 represents the initial *I–V* curve of the modified cell frame with standard and corroded cell frames as references.

When H_2 was used as a fuel, Ni-electroplated cell frame performed well as the standard cell frame (Fig. 6(a)). As a note, even the corroded cell frame which was exposed for 2000 h showed good result. However, Ni electroless plated cell frame, which should act as corrosion resistance cell frame, showed the lowest performance of all. All OCV values corresponded one another, which meant that there were no changes in gas composition due to the modification of cell frame [9].

However, when bio-ethanol was used as a fuel, significant change in OCV was observed on the Ni electroless plated cell frame (Fig. 6(b)). The gas output composition suggested low H_2 content in this case, which may have resulted from the poisoning of the Ni/MgO reforming catalyst. The highest performance was achieved by the Ni-electroplated cell frame, followed in order by standard and corroded cell frame with a slight difference. The Ni on the electroplated cell frame not only acted as corrosion resistance layer, but also as a catalyst for steam reforming of bio-ethanol [10–15]. This explained the increase in performance compared with the performance of standard or corroded cell frames. The slope difference between *I–V* curves in Fig. 6(a) and (b) is due to the different capabilities to enact electrochemical reaction in H_2 or in bio-ethanol atmosphere. Fig. 6(b) shows steep slopes that suggest insufficient H_2 produced by steam reforming of bio-ethanol at high current density to carry out electrochemical reaction in MCFC.

Further study revealed the reason for those odd phenomena. All single cells were operated for over 1000 h (Fig. 7). There was a considerable difference in the voltage loss, as can be seen in Table 3. The decrease in OCV occurred due to electrolyte poisoned on the Ni/MgO reforming catalyst. The electrolyte was redistributed because of corrosion on the wet seal area. Consequently, the loss of electrolyte became higher when the oxide layer spread out.

Post test data revealed that Ni electroless and corroded cell frames had high voltage drop and electrolyte loss. The loss of electrolyte affected the cell performance, since the number of active sites, in this case triple phase boundaries, was limited [11,15–18]. The SEM images and pore size distribution curves of the anodes after 1000 h operation illustrated the loss of porosity in Ni electroless plated cell frame (Figs. 8 and 9).

ICP-AES analysis revealed that Ni electroless plated cell frame consisted of 92 wt% of Ni and 8 wt% of P. The chemical reaction for electroless plating method is as follows:

$$NiSO_4 + 2NaH_2PO_2 + 2H_2O \rightarrow Ni + 2NaHPO_3 + H_2 + H_2SO_4$$

It seemed that there was P content remaining, which could not be fully removed even after heat treated at 650 °C. The

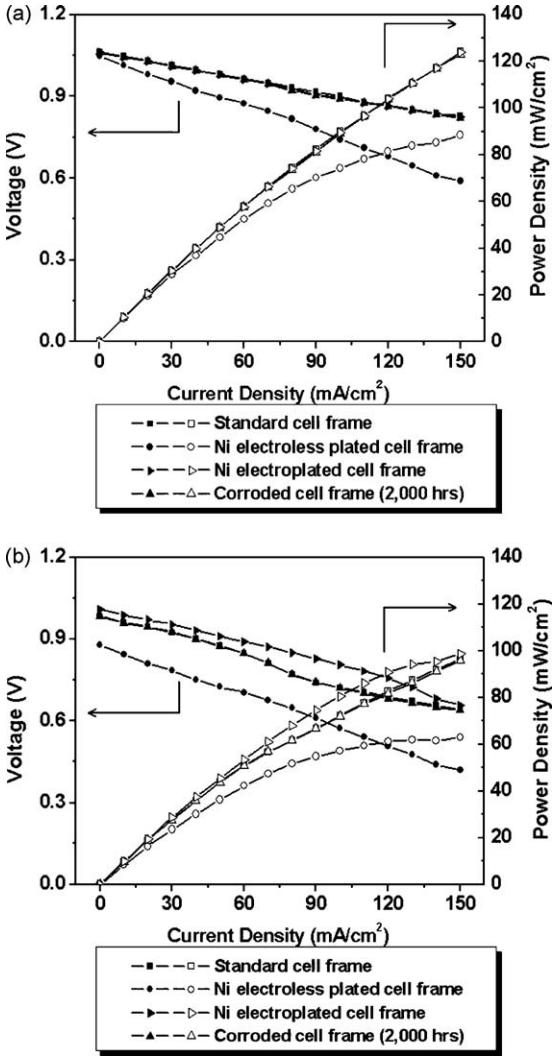

Fig. 6. Initial *I–V* curve of various cell frames with (a) H_2 and (b) bio-ethanol as a fuel.

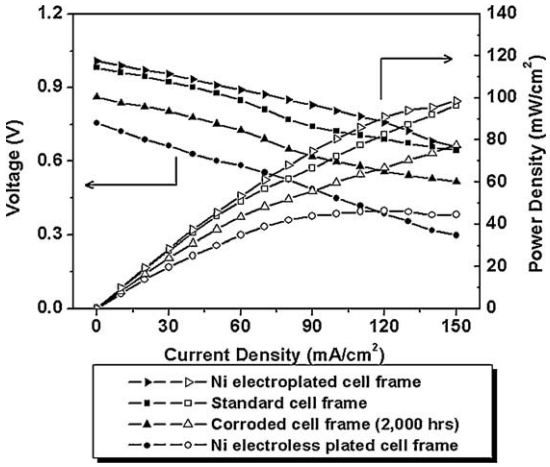

Fig. 7. *I–V* curve of various modified cell frame after 1000 h operation.

Table 3
Voltage loss of various modification cell frames.

Sample	Voltage loss (mV/1000 h)	Electrolyte loss (wt%)
Ni electroplated cell frame	7	3.7
Standard cell frame	9	3.9
Ni electroless cell frame	121	22.1
Corroded cell frame	110	21.0

phosphorous from Ni electroless plating accelerated the rate of corrosion, resulting in low performance. Corrosion rate of stainless steel increases with the increase in phosphorus content [5,19–24]. The corrosion withdrew the electrolyte and decreased the triple phase boundary resulting in low voltage at 150 mA/cm^2 under H_2 atmosphere (Fig. 6(a)). Eventually, the electrolyte came in contact with the reforming catalyst, reducing the amount of active sites to

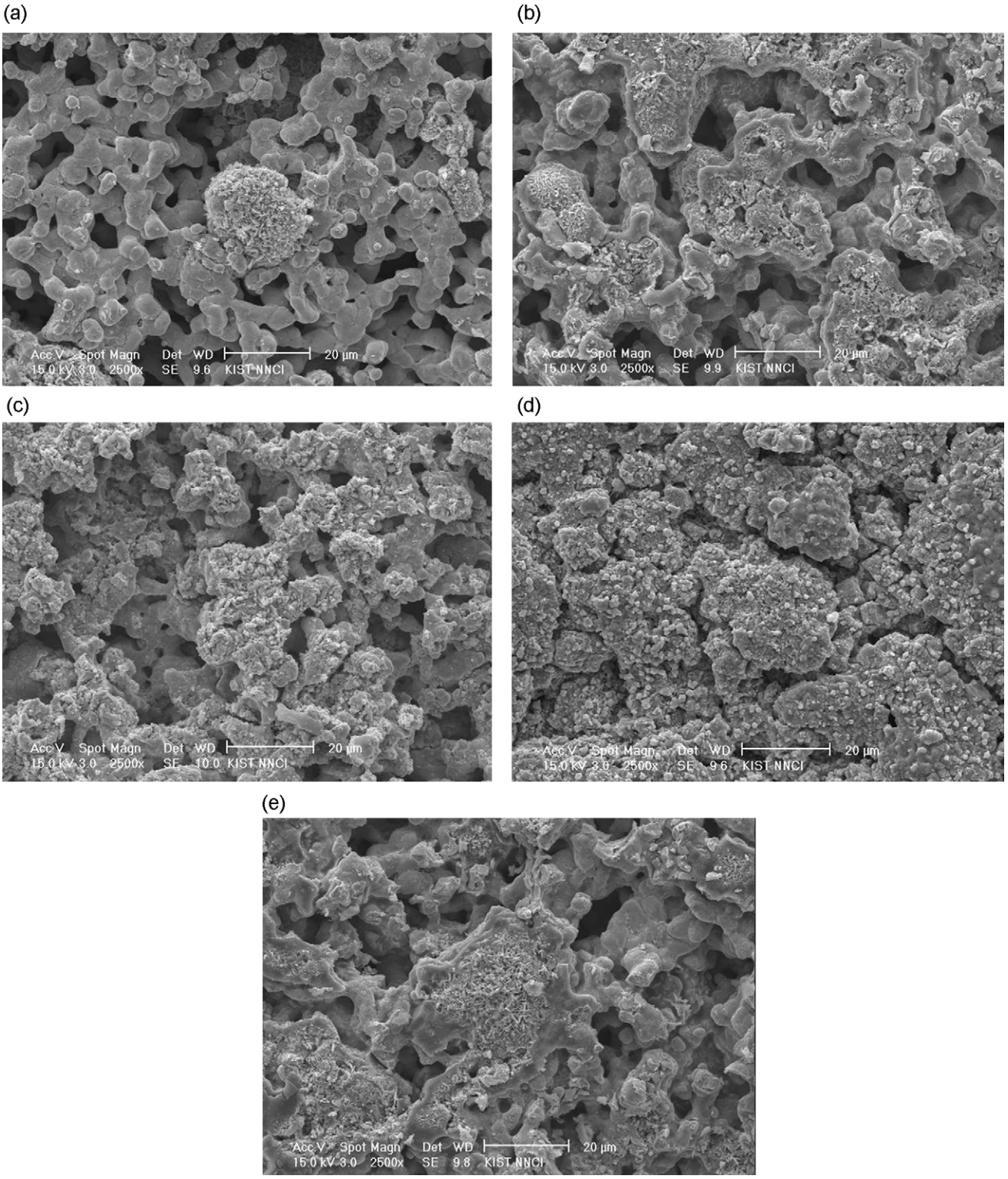

Fig. 8. SEM images of anode (a) as-prepared, (b) with standard cell frame, (c) with Ni electroplated cell frame, (d) with electroless plated cell frame, and (e) with 2000 h corroded cell frame after 1000 h operation.

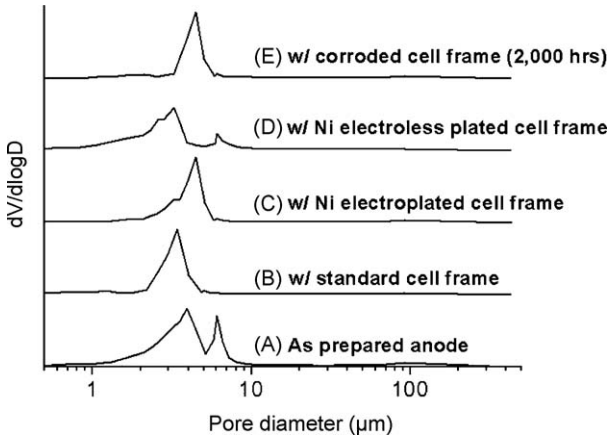

Fig. 9. Pore size distribution of anode after 1000 h operation.

yield low H_2 selectivity. This phenomenon was recorded as low performance of Ni electroless plated anode.

Corroded cell frame also showed high voltage drop across the cell and electrolyte loss; however, the reason is different since there is no phosphorus content in the corroded cell frame. Additional set of experiments explained that an increase in ohmic loss occurred after 400 h (Fig. 10). The initial amount of electrolyte in corroded cell frame was more than enough to carry out electrochemical reaction at 150 mA/cm^2. However, the continuous electrolyte migration to the corroded area eventually broke the barrier, thus a linear increase in ohmic resistance was detected after 400 h (Fig. 11). In other words, the corroded cell frame started to loose its electrolyte by the sudden increase in ohmic resistance [25–28].

The highest performance was achieved when Ni-electroplating was used to prevent cell frame corrosion. Ni was able to protect the stainless steel surface from the corrosion. The initial performance of Ni-electroplating cell frame was almost similar to that of the standard cell frame when H_2 was used as a fuel. However, for bio-ethanol, this Ni layer had dual functions. The first one was acting as corrosion resistance layer, and the second one as bio-ethanol reforming catalyst [29–33]. These advantages of the Ni-electroplating together with the previous mentioned recycling system are the most suitable modification for direct bio-ethanol reforming MCFC system.

Some researchers argued about Ni-coated cell frame. In one point of view, Ni can prevent stainless steel from corrosion since Ni is thermodynamically stable in the anode gas atmosphere [10].

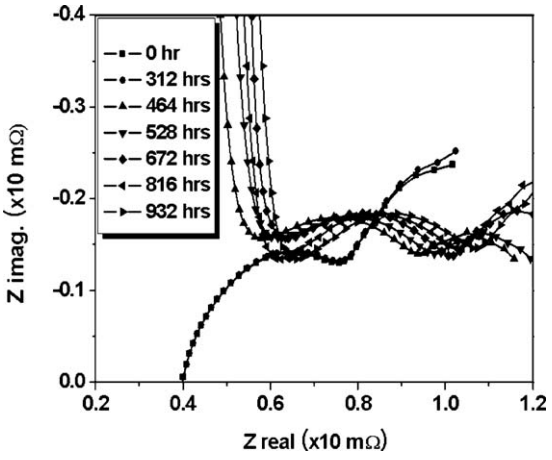

Fig. 10. EIS spectra of corroded cell frame towards time.

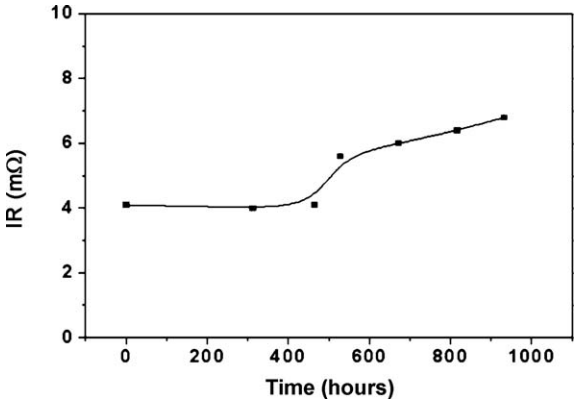

Fig. 11. Ohmic resistance of corroded cell frame as a function of time.

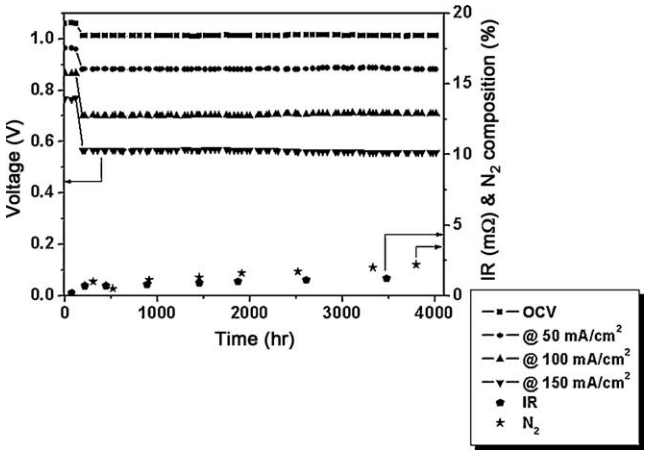

Fig. 12. Long term operation of single cell after modification.

However, others debated that coke formation on Ni due to high solubility and diffusivity of carbon is a well-known reason of the deactivation of Ni-containing catalysts for steam reforming. Furthermore, it may cause the damage of stainless steel cell frame [9,10].

In this system, the use of bio-ethanol as a fuel brings additional advantage. The so-called bio-ethanol consists of huge amount of water (mole H_2O/mole EtOH = 13). This amount of water makes the system stay at the outside of the carbon deposition region [34,35]. Even under recycling system, the anode chamber still maintains sufficient amount of water to avoid carbon formation.

In other words, the corrosion resistance and high performance of Ni-electroplating cell were achieved successfully due to the thermodynamically stable Ni layer that protected SS316L cell frame from corrosion and simultaneously acted as a catalyst for steam reforming of bio-ethanol without any carbon deposition problem because of high water to ethanol ratio, respectively.

In addition, the single cell modified with recycling system and Ni electroplated cell frame was successfully tested for 4000 h without any significant decrease in performance, as can be seen in Fig. 12.

4. Conclusions

The increase in water partial pressure decreased the initial single cell performance. The optimum recycling ratio was achieved at the range between 0.7 and 1 when H_2O and H_2 concentrations were in the optimum condition. Ni electroless plating did not show

any resistance against corrosion due to the impurity from P species during the coating process. Ni electroplating successfully acted as a corrosion resistant as well as a reforming catalyst in bio-ethanol atmosphere.

Acknowledgements

This work was financially supported by Center for Fuel Cell Research of Korea Institute of Science and Technology, and by the ERC program of MOST/KOSEF (Grant No. R11-2002-102-00000-0).

References

[1] J. Larminie, A. Dicks, Fuel Cell System Explained, 2nd ed., 2003.
[2] H. Devianto, S.-Y. Kim, H.-C. Hahm, J. Han, S.W. Nam, T.-H. Lim, H.-I. Lee, Proc. 212th Electrochem. Soc. Meeting, 2007, p. 47.
[3] J.P.P. Huijsmans, G.J. Kraaij, R.C. Makkus, G. Rietveld, E.F. Sitters, H.T.J. Reijers, J. Power Sources 86 (2000) 117.
[4] R.A. Donado, L.G. Marianowski, H.C. Maru, J.R. Selman, J. Electrochem. Soc. 131 (1984) 2541.
[5] G. Lindbergh, B. Zhu, Electrochim. Acta 46 (2001) 1131.
[6] J.H. Wee, D.J. Song, C.S. Jun, T.-H. Lim, S.A. Hong, H.C. Lim, K.Y. Lee, J. Alloys Compd. 390 (2005) 155.
[7] S.P. Yoon, J. Han, S.W. Nam, T.-H. Lim, I.-H. Oh, H. Devianto, H.-I. Lee, H.C. Hahm, Y.C. Kim, Korea Patent 803,669 (2008).
[8] H.J. Cleary, N.D. Greene, Corr. Sci. 7 (1967) 821.
[9] S. Freni, S. Cavallaro, M. Aquino, D. Ravida, N. Giordano, Int. J. Hydrogen Energy 19 (1994) 337.
[10] S. Frangini, J. Power Sources 182 (2008) 462.
[11] J.-H. Kim, H.-J. Kim, T.-H. Lim, H.-I. Lee, J. Ind. Eng. Chem. 13 (2007) 850.
[12] S. Randstrom, C. Lagergren, P. Capobianco, J. Power Sources 160 (2006) 782.
[13] K. Sugiura, T. Yodo, M. Yamauchi, K. Tanimoto, J. Power Sources 157 (2006) 739.
[14] G. Durante, S. Vegni, P. Capobianco, F. Golgovic, J. Power Sources 152 (2005) 204.
[15] K. Sugiura, M. Yamauchi, K. Tanimoto, Y. Yoshitani, J. Power Sources 145 (2005) 199.
[16] B. Zhu, G. Lindbergh, D. Simonsson, Corr. Sci. 41 (1999) 1497.
[17] J.G. Seo, M.H. Youn, H.-I. Lee, J.J. Kim, E. Yang, J.S. Chung, P. Kim, I.K. Song, Chem. Eng. J. 141 (2008) 298.
[18] B. Zhu, G. Lindbergh, D. Simonsson, Corr. Sci. 41 (1999) 1515.
[19] P. Biedenkopf, M. Spiegel, H.J. Grabke, Electrochim. Acta 44 (1998) 683.
[20] S.H. Kim, S.W. Nam, T.-H. Lim, H.-I. Lee, Appl. Catal. B: Environ. 81 (2008) 97.
[21] M. Keijzer, K. Hemmes, P.J.J.M. Van Der Put, J.H.W. De Wit, J. Schoonman, Corr. Sci 39 (1997) 483.
[22] F. Yoshiba, Y. Izaki, T. Watanabe, J. Power Sources 132 (2004) 52.
[23] F. Yoshiba, N. Ono, Y. Izaki, T. Watanabe, T. Abe, J. Power Sources 71 (1998) 328.
[24] M. Benito, J.L. Sanz, R. Isabel, R. Padilla, R. Arjona, L. Daza, J. Power Sources 151 (2005) 11.
[25] S. Freni, S. Cavallaro, N. Mondello, L. Spadaro, F. Frusteri, J. Power Sources 108 (2002) 53.
[26] K. Sugiura, I. Naruse, J. Power Sources 106 (2002) 51.
[27] H.-K. Park, Y.-R. Lee, M.-H. Kim, G.-Y. Chung, S.W. Nam, S.-A. Hong, T.-H. Lim, H.-C. Lim, J. Power Sources 104 (2002) 140.
[28] M.-H. Kim, H.-K. Park, G.-Y. Chung, H.-C. Lim, S.W. Nam, T.-H. Lim, S.-A. Hong, J. Power Sources 103 (2002) 245.
[29] S.H. Clarke, A.L. Dicks, K. Pointon, T.A. Smith, A. Swann, Catal. Today 38 (1997) 411.
[30] J.C. Vargas, S. Libs, A.-C. Roger, A. Kiennemann, Catal. Today 107 (2005) 417.
[31] P. Yaseneva, S. Pavlova, V. Sadykov, G. Alikina, A. Lykashevich, V. Rogov, S. Belochapkine, J. Ross, Catal. Today 137 (2008) 23.
[32] H. Song, L. Zhang, R.B. Watson, D. Braden, U.S. Ozkan, Catal. Today 129 (2007) 346.
[33] A.N. Fatsikostas, D.I. Kondarides, X.E. Verykios, Catal. Today 75 (2002) 145.
[34] V. Mas, R. Kipreos, N. Amadeo, M. Laborde, Int. J. Hydrogen Energy 31 (2006) 21.
[35] K. Sasaki, K. Watanabe, Y. Teraoka, J. Electrochem. Soc. 151 (2004) A965.